J|A|C|S
ARTICLES
Published on Web 02/26/2002

Definitive Evidence for Monoanionic Binding of 2,3-Dihydroxybiphenyl to 2,3-Dihydroxybiphenyl 1,2-Dioxygenase from UV Resonance Raman Spectroscopy, UV/Vis Absorption Spectroscopy, and Crystallography

Frédéric H. Vaillancourt,*,† Christopher J. Barbosa,*,‡,§ Thomas G. Spiro,|| Jeffrey T. Bolin,⊥ Michael W. Blades,‡ Robin F. B. Turner,*,§,# and Lindsay D. Eltis*,†

Contributions from the Departments of Biochemistry and Microbiology, The University of British Columbia, 300-6174 University Boulevard, Vancouver, B.C., V6T 1Z3, Canada; Department of Chemistry, The University of British Columbia, E257-2036 Main Mall, Vancouver, B.C., V6T 1Z1, Canada; Biotechnology Laboratory, The University of British Columbia, 237-6174 University Boulevard, Vancouver, B.C., V6T 1Z3, Canada; Department of Chemistry, Princeton University, Princeton, New Jersey 08544; Department of Biological Sciences, Purdue University, West Lafayette, Indiana 47907-1392; and Department of Electrical Engineering, The University of British Columbia, 434-2356 Main Mall, Vancouver, B.C., V6T 1Z4, Canada

Received November 5, 2001

Abstract: Ultraviolet resonance Raman spectroscopy (UVRRS), electronic absorption spectroscopy, and X-ray crystallography were used to probe the nature of the binding of 2,3-dihydroxybiphenyl (DHB) to the extradiol ring-cleavage enzyme, 2,3-dihydroxybiphenyl 1,2-dioxygenase (DHBD; EC 1.13.11.39). The lowest lying transitions in the electronic absorption spectrum of DHBD-bound DHB occurred at 299 nm, compared to 305 nm for the monoanionic DHB species in buffer. In contrast, the corresponding transitions in neutral and dianionic DHB occurred at 283 and 348 nm, respectively, indicating that DHBD-bound DHB is monoanionic. These binding-induced spectral changes, and the use of custom-designed optical fiber probes, facilitated UVRR experiments. The strongest feature of the UVRR spectrum of DHB was a Y8a-like mode around 1600 cm^{-1}, whose position depended strongly on the protonation state of the DHB. In the spectrum of the DHBD-bound species, this feature occurred at 1603 cm^{-1}, as observed in the spectrum of monoanionic DHB. Raman band shifts were observed in deuterated solvent, ruling out dianionic binding of the substrate. Thus, the electronic absorption and UVRRS data demonstrate that DHBD binds its catecholic substrate as a monoanion, definitively establishing this feature of the proposed mechanism of extradiol dioxygenases. This conclusion is supported by a crystal structure of the DHBD:DHB complex at 2.0 Å resolution, which suggests that the substrate's 2-hydroxyl substituent, and not the 3-hydroxyl group, deprotonates upon binding. The structural data also show that the aromatic rings of the enzyme-bound DHB are essentially orthogonal to each other. Thus, the 6 nm blue shift of the transition for bound DHB relative to the monoanion in solution could indicate a conformational change upon binding. Catalytic roles of active site residues are proposed based on the structural data and previously proposed mechanistic schemes.

Introduction

The microbial aerobic degradation of aromatic compounds generally proceeds via a catecholic catabolite with hydroxyl substituents on two adjacent carbon atoms. Such compounds are cleaved by dioxygenases from one of two distinct classes. Intradiol dioxygenases cleave the bond situated between the two hydroxyl groups and typically depend on mononuclear non-heme Fe(III). In contrast, extradiol dioxygenases cleave a bond adjacent to the two hydroxyl groups and typically depend on mononuclear non-heme Fe(II). Although these distinctions may appear to be minor, they are in fact a manifestation of enzymes that have completely different structures and utilize different catalytic mechanisms (see recent reviews[1−3]).

Extradiol dioxygenases have been divided into two classes based on primary and tertiary structural data.[4,5] The ferrous iron of these enzymes is coordinated by two histidines and one

* Corresponding authors: Robin F. B. Turner, robint@ee.ubc.ca. Lindsay D. Eltis, leltis@interchange.ubc.ca.
† Departments of Biochemistry and Microbiology, The University of British Columbia.
‡ Department of Chemistry, The University of British Columbia.
§ Biotechnology Laboratory, The University of British Columbia.
|| Princeton University.
⊥ Purdue University.
Department of Electrical Engineering, The University of British Columbia.

(1) Que, L., Jr.; Ho, R. Y. N. *Chem. Rev.* **1996**, *96*, 2607−2624.
(2) Solomon, E. I.; Brunold, T. C.; Davis, M. I.; Kemsley, J. N.; Lee, S.-K.; Lehnert, N.; Neese, F.; Skulan, A. J.; Yang, Y.-S.; Zhou, J. *Chem. Rev.* **2000**, *100*, 235−349.
(3) Bugg, T. D. H.; Lin, G. *Chem. Commun.* **2001**, *2001*, 941−952.
(4) Eltis, L. D.; Bolin, J. T. *J. Bacteriol.* **1996**, *178*, 5930−5937.

glutamate[6] in what has been termed the 2-His-1-carboxylate facial triad motif.[7] This ferrous center has a square pyramidal geometry,[8] with an axially coordinated histidine and two solvent species as the other basal ligands.[6] In the first step of the proposed mechanism, bidentate binding of the catecholic substrate displaces the two solvent ligands of the ferrous iron[8−12] and activates the latter for O_2 binding.[8,9,13] Subsequent steps in the catalytic mechanism are less well substantiated. Biochemical studies provide some support for a mechanism involving iron-mediated transfer of an electron from the catechol to the O_2, yielding a semiquinone−Fe(II)−superoxide intermediate.[14] This species is proposed to react to give an iron−alkylperoxo intermediate,[15] which undergoes alkenyl migration, Criegee rearrangement, and O−O bond cleavage to give an unsaturated lactone intermediate and an Fe(II)-bound hydroxide ion. The latter hydrolyzes the lactone to yield the reaction product.[16]

The intradiol family of dioxygenases include protocatechuate 3,4-dioxygenases (3,4-PCD; EC 1.13.11.3), which cleave hydroxybenzoates, and catechol 1,2-dioxygenases (C12O; EC 1.13.11.1), which cleave catechols and hydroxyquinols. The ferric iron of substrate-free intradiol dioxygenase has a distorted trigonal bipyramid geometry, with a tyrosine, a histidine, and a solvent species coordinated in the equatorial plane and a tyrosine and a histidine coordinated in the axial positions.[17] As in extradiol dioxygenases, the intradiol enzymes utilize an ordered mechanism in which substrate binding precedes O_2 reactivity.[18−20] Substrate-binding is a multistep process that ultimately results in displacement of an axial tyrosine and an equatorial hydroxide ion to yield a bidentate bound catecholate.[21−25] In the proposed mechanism, O_2 attacks the bound substrate directly, before coordinating to the iron and yielding an iron−alkylperoxo intermediate.[26] Although recent evidence indicates that this intermediate is similar in structure to that of the extradiol reaction,[15] in the case of intradiol enzymes, the Criegee rearrangement and O−O bond cleavage involve acyl migration to yield the cyclic anhydride and an iron-bound oxide or hydroxide. The latter functions as a nucleophile to hydrolyze the anhydride and yield the ring-opened product. The stereoelectronic factors that determine extradiol versus intradiol cleavage from the common intermediate have been proposed to involve the orientation of the iron−alkylperoxo moiety relative to the organic substrate (pseudoaxial versus pseudoequatorial[3]).

An important difference in the initial stages of the proposed extradiol and intradiol mechanisms is the protonation state of the bidentate-bound catechol in the enzyme:substrate complex.[1] Thus, in extradiol dioxygenases, a monoanionic Fe(II)-bound catecholate activates the ferrous center for O_2-binding.[13] By contrast, in intradiol dioxygenases, a dianionic Fe(III)-bound catecholate promotes direct electrophilic attack of the substrate by O_2, a reaction that is further favored by ketonization of the catecholate.[26] Despite the proposed significance of the different protonation states of the substrate in the two enzymes, the evidence for these respective states is not definitive. Thus, structural and EXAFS data demonstrate that in both enzymes, the substrate is asymmetrically bound: one Fe−O bond is shorter than the other. This has been interpreted as a ketonized dianion in the case of intradiol dioxygenases[22,24,27] and as a monoanion in the case of extradiol dioxygenases.[11−13] Electronic absorption and resonance Raman data supporting these interpretations were obtained using poor substrates or inhibitors[27−29] which may not bind in the same manner as preferred substrates. Additional evidence for monoanionic binding in extradiol dioxygenases is provided by a model reaction using a ferrous complex of 1,4,7-triazacyclononane in which extradiol cleavage apparently required a monoanionic catecholate substrate.[30]

In this study, the binary complex between 2,3-dihydroxybiphenyl 1,2-dioxygenase (DHBD; EC 1.13.11.39) from *Burkholderia* sp. LB400 and 2,3-dihydroxybiphenyl (DHB) was studied using UV/Vis absorption spectroscopy, ultraviolet resonance Raman spectroscopy (UVRRS), and X-ray crystallography. Raman spectroscopy in general has undergone enormous growth as a tool for studying biological samples, and UVRRS in particular has made important contributions to the understanding of protein dynamics.[31−33] UVRRS has also been used to study the interaction of substrates and inhibitors with various proteins[34−38] to reveal detailed information about hydrogen bonding and hydrophobic interactions. A unique fiber-optic-coupled UVRR spectrometer was used to enable the rapid acquisition of high quality spectra[39] of the photolabile enzyme

(5) Sugimoto, K.; Senda, T.; Aoshima, H.; Masai, E.; Fukuda, M.; Mitsui, Y. *Structure* **1999**, *7*, 953−965.
(6) Han, S.; Eltis, L. D.; Timmis, K. N.; Muchmore, S. W.; Bolin, J. T. *Science* **1995**, *270*, 976−980.
(7) Hegg, E. L.; Que, L., Jr. *Eur. J. Biochem.* **1997**, *250*, 625−629.
(8) Mabrouk, P. A.; Orville, A. M.; Lipscomb, J. D.; Solomon, E. I. *J. Am. Chem. Soc.* **1991**, *113*, 4053−4061.
(9) Arciero, D. M.; Orville, A. M.; Lipscomb, J. D. *J. Biol. Chem.* **1985**, *260*, 14035−14044.
(10) Arciero, D. M.; Lipscomb, J. D. *J. Biol. Chem.* **1986**, *261*, 2170−2178.
(11) Vaillancourt, F. H.; Han, S.; Fortin, P. D.; Bolin, J. T.; Eltis, L. D. *J. Biol. Chem.* **1998**, *273*, 34887−34895.
(12) Uragami, Y.; Senda, T.; Sugimoto, K.; Sato, N.; Nagarajan, V.; Masai, E.; Fukuda, M.; Mitsui, Y. *J. Inorg. Biochem.* **2001**, *83*, 269−279.
(13) Shu, L.; Chiou, Y.-M.; Orville, A. M.; Miller, M. A.; Lipscomb, J. D.; Que, L., Jr. *Biochemistry* **1995**, *34*, 6649−6659.
(14) Spence, E. L.; Langley, G. J.; Bugg, T. D. H. *J. Am. Chem. Soc.* **1996**, *118*, 8336−8343.
(15) Winfield, C. J.; Al-Mahrizy, Z.; Gravestock, M.; Bugg, T. D. H. *J. Chem. Soc., Perkin Trans. 1* **2000**, *2000*, 3277−3289.
(16) Sanvoisin, J.; Langley, G. J.; Bugg, T. D. H. *J. Am. Chem. Soc.* **1995**, *117*, 7836−7837.
(17) Ohlendorf, D. H.; Lipscomb, J. D.; Weber, P. C. *Nature* **1988**, *336*, 403−405.
(18) Hori, K.; Hashimoto, T.; Nozaki, M. *J. Biochem.* **1973**, *74*, 375−384.
(19) Bull, C.; Ballou, D. P.; Otsuka, S. *J. Biol. Chem.* **1981**, *256*, 12681−12686.
(20) Walsh, T. A.; Ballou, D. P.; Mayer, R.; Que, L., Jr. *J. Biol. Chem.* **1983**, *258*, 14422−14427.
(21) True, A. E.; Orville, A. M.; Pearce, L. L.; Lipscomb, J. D.; Que, L., Jr. *Biochemistry* **1990**, *29*, 10847−10854.
(22) Orville, A. M.; Lipscomb, J. D.; Ohlendorf, D. H. *Biochemistry* **1997**, *36*, 10052−10066.
(23) Frazee, R. W.; Orville, A. M.; Dolbeare, K. B.; Yu, H.; Ohlendorf, D. H.; Lipscomb, J. D. *Biochemistry* **1998**, *37*, 2131−2144.
(24) Vetting, M. W.; D'argenio, D. A.; Ornston, L. N.; Olhendorf, D. H. *Biochemistry* **2000**, *39*, 7943−7955.
(25) Vetting, M. W.; Ohlendorf, D. H. *Structure* **2000**, *8*, 429−440.
(26) Que, L., Jr.; Lipscomb, J. D.; Munck, E.; Wood, J. M. *Biochim. Biophys. Acta* **1977**, *485*, 60−74.
(27) Elgren, T. E.; Orville, A. M.; Kelly, K. A.; Lipscomb, J. D.; Ohlendorf, D. H.; Que, L., Jr. *Biochemistry* **1997**, *36*, 11504−11513.
(28) Tyson, C. A. *J. Biol. Chem.* **1975**, *250*, 1765−1770.
(29) Que, L., Jr.; Epstein, R. M. *Biochemistry* **1981**, *20*, 2545−2549.
(30) Lin, G.; Reid, G.; Bugg, T. D. H. *J. Am. Chem. Soc.* **2001**, *123*, 5030−5039.
(31) Lednev, I. K.; Karnoup, A. S.; Sparrow, M. C.; Asher, S. A. *J. Am. Chem. Soc.* **1999**, *121*, 4076−4077.
(32) Hu, X.; Rodgers, K. R.; Mukerji, I.; Spiro, T. G. *Biochemistry* **1999**, *38*, 3462−3467.
(33) Thomas, G. J. *Annu. Rev. Biophys. Biomol. Struct.* **1999**, *28*, 1−27.
(34) Hashimoto, S.; Yabusaki, T.; Takeuchi, H.; Harada, I. *Biospectroscopy* **1995**, *1*, 375−385.
(35) Austin, J. C.; Kuliopulos, A.; Mildvan, A. S.; Spiro, T. G. *Protein Sci.* **1992**, *1*, 259−270.
(36) Couling, V. W.; Fischer, P.; Klenerman, D.; Huber, W. *Biophys. J.* **1998**, *75*, 1097−1106.
(37) Wilson, K. J.; McNamee, M. G.; Peticolas, W. L. *J. Biomol. Struct. Dyn.* **1991**, *9*, 489−509.
(38) Efremov, R. G.; Feofanov, A. V.; Dzhandzhugazyan, K. N.; Modyanov, N. N.; Nabiev, I. R. *FEBS Lett.* **1990**, *260*, 257−260.

and substrate. Spectra of the enzyme:substrate (ES) complex were analyzed through comparison with the spectra of free DHB in its three different ionization states in protonated and deuterated buffers. The spectroscopic and crystallographic results are discussed in terms of the proposed catalytic mechanism of extradiol dioxygenases.

Experimental Section

Chemicals. Catechol, biphenyl, sodium methoxide, sodium *tert*-butoxide, sodium hydrosulfite, and *tert*-butyl alcohol were from Sigma-Aldrich (Mississauga, Ontario, Canada). Deuterium oxide, sodium deuterioxide, methanol-OD, and *tert*-butyl alcohol-OD were from Cambridge Isotope Laboratories (Andover, MA) or from C/D/N Isotopes (Pointe-Claire, Quebec, Canada). 2,3-DHB[40] was a gift from Dr. Victor Snieckus (Department of Chemistry, Queens University, Kingston, Ontario, Canada). Ferene-S was from ICN Biomedicals Inc. (Aurora, OH). All other chemicals were of analytical grade and used without further purification.

Preparation of Samples. Buffers were prepared using water purified on a Barnstead NANOpure UV apparatus to a resistivity of greater than 17 MΩ·cm. Samples for spectroscopy and titrations were prepared under an inert atmosphere unless otherwise specified, usually in a Mbraun Labmaster 100 glovebox (Newburyport, MA) maintained at less than 1 ppm O_2. Buffers and solvents were vigorously bubbled with argon for 20 min, brought into the glovebox, and allowed to equilibrate for 24 h prior to use. DHB and catechol were weighed in small glass vials (Wheaton, Millville, NJ) and transferred to the glovebox for sample preparation. DHBD was purified chromatographically and flash frozen in liquid nitrogen for long-term storage as described previously.[11] Aliquots of DHBD (500−700 μL) were transferred to the glovebox, thawed immediately prior to use, and exchanged into 20 mM Tris, pH 8.0, by gel filtration chromatography using a 1.5 cm × 8 cm column of Biogel P6 DG (Bio-Rad, Mississauga, Ont., Canada). The ES complex was prepared by combining DHB with a slight molar excess of DHBD (ratios between 1:1.2 and 1:2). Samples for UVRRS also contained 100 mM Na_2SO_4 and, if DHBD was present, 10 μM sodium hydrosulfite. Samples for spectroscopy were transferred to the appropriate sealed cuvettes and removed from the glovebox. Protein concentrations were determined by the Bradford method.[41] Iron concentrations were determined colorimetrically using Ferene S.[42]

UV/Vis Absorption Spectroscopy. Spectra were recorded using a Varian Cary 1E spectrophotometer equipped with a thermostated cuvette holder (Varian Canada, Mississauga, Ontario, Canada) set at 25 °C. The spectrophotometer was interfaced to a microcomputer and controlled by Cary WinUV software version 2.00. A 1-mL gastight cuvette (Hellma, Concord, Ontario, Canada) was used for anaerobic samples of catecholic compounds prepared in the absence and presence of DHBD. A conventional 1-mL cuvette was used for activity assays.

UV Resonance Raman Spectroscopy. The UVRR spectrometer employed an intracavity frequency-doubled argon-ion laser (Innova 90C FreD, Coherent Inc., Santa Clara, CA) operated at 248.2 nm except for measurement of the resonance enhancement profile where data were also collected at 229.0, 238.2, 244.0, 250.8, and 257.2 nm. Light was transmitted and collected via in-house built fiber-optic probes specifically designed for use with resonance Raman spectroscopy.[39,43,44] The Raman scatter was dispersed by a 0.67 m monochromator (Model 207, MacPherson Inc., Chelmsfod, MA) with a 3600 groove/mm grating. A dielectric stack interference filter (Barr Associates, Westford, MA) was employed before the slit for Rayleigh line rejection, and the dispersed signal was collected with a thermoelectrically cooled CCD camera (SpectraVideo, Pixelvision Inc., Tigard, OR) interfaced with a personal computer running PixelView software (Pixelvision Inc.). Further manipulations of the data, including wavenumber calibration, averages, and dynamic subtractions, were performed using Grams32 software (Thermo Galactic, Salem, NH).

UVRRS was performed using a 1.5-mL centrifuge tube containing ∼200 μL of material. Samples containing neutral or monoanionic catecholic species were maintained under argon upon removal from the glovebox. Samples containing dianionic species or DHBD were flash frozen in liquid nitrogen upon removal from the glovebox. Immediately prior to data acquisition, the sample cuvette was fitted with the fiber optic probe, maintained under a continuous flow of argon, and washed with a solution of 2 mM sodium hydrosulfite using a gastight syringe. Samples were thawed and/or transferred to the cuvette under argon. Samples were stirred continuously and were exposed to no more than three 10-s acquisitions of 20 mW, illuminating a circular area of ∼0.28 mm^2. This results in a flux density of ∼7 W/cm^2, which is well below accepted levels for conventional UVRR spectrometers.[39] The resulting spectra were retained only if the acquisitions were internally consistent as determined by subtracting the different acquisitions from each other. For these comparisons, the 982 cm^{-1} peak of sulfate (in aqueous solution) or the organic solvent peaks were used as internal standards. In addition, spectra of protein samples were discarded if the sample lost more than 15% of its initial DHBD activity as determined by assaying the activity in 10 μL aliquots withdrawn from the cuvette after each 10-s acquisition.

Activity Measurements. Enzymatic activity was measured by spectrophotometrically following the rate of appearance of yellow-colored ring-cleaved product at 434 nm ($\epsilon = 25.7\ mM^{-1}\ cm^{-1}$). Initial velocities were determined from progress curves by analyzing the data using the Cary WinUV software. The slope of the progress curve and the correlation coefficient of the slope were calculated for the first 6 s of the assay. The activity assay was performed in a total volume of 1.0 mL of air-saturated 20 mM HEPPS, 80 mM NaCl ($I = 0.1$ M), pH 8.0, 25.0 ± 0.1 °C containing 80 μM DHB. The reaction was initiated by injecting between 2 and 10 μL of an appropriate dilution of enzyme preparation into the cuvette. Enzyme dilutions were prepared and manipulated as previously described.[11]

Titration Curves. The first pK_a values for catechol and DHB were determined using a model PHM93 Reference pH Meter (Radiometer, Copenhagen, Denmark) mounted in the glovebox. Catechol and DHB were dissolved in deionized water to final concentrations of 50 mM and 25 mM, respectively. Each compound was titrated by adding microliter volumes of an equimolar solution of NaOH.

Crystallographic Procedures. Typical procedures for the preparation of crystals and execution of diffraction experiments under anaerobic conditions, as well as for model building and refinement, have been described previously, together with a summary of the diffraction data.[11] In brief, crystals of the binary complex of DHBD and DHB were prepared by incubation for ∼8 h at 4 °C in a solution containing 1 mM DHB, 22% (w/v) PEG-4000, 15% (v/v) *tert*-butyl alcohol, and 100 mM HEPES buffer at pH 7.5. The diffraction data were measured at 20 °C from one crystal to 2.0 Å resolution by the rotation method using an imaging plate area detector (R-axis IIC, Molecular Structures Corporation) and Cu−Kα radiation (Rigaku RU200 generator) conditioned by bent mirror optics (Molecular Structures Corporation).

Enzyme:DHB crystals were essentially isomorphous to those of the substrate-free enzyme. Refinement was initiated using the substrate-free structure[6] with nonprotein atoms (Fe, water, and *tert*-butyl alcohol) from the vicinity of the active site deleted. The active site Fe and DHB were then added by interpretation of $|F_o| - |F_c|$ difference maps. Following additional computational refinement, active site water molecules and an adventitiously bound *tert*-butyl alcohol[11] were added

(39) Barbosa, C. J.; Vaillancourt, F. H.; Eltis, L. D.; Blades, M. W.; Turner, R. F. B. *J. Raman Spectrosc.* **2002**, *33*, in press.
(40) Nerdinger, S.; Kendall, C.; Marchhart, R.; Riebel, P.; Johnson, M. R.; Yin, C.-F.; Eltis, L. D.; Snieckus, V. *Chem. Commun.* **1999**, *1999*, 2259−2260.
(41) Bradford, M. M. *Anal. Biochem.* **1976**, *72*, 248−254.
(42) Haigler, B. E.; Gibson, D. T. *J. Bacteriol.* **1993**, *172*, 457−464.
(43) Greek, L. S.; Schulze, H. G.; Haynes, C. A.; Blades, M. W.; Turner, R. F. B. *Appl. Opt.* **1996**, *35*, 4086−4095.
(44) Greek, L. S.; Schulze, H. G.; Blades, M. W.; Haynes, C. A.; Klein, K. F.; Turner, R. F. B. *Appl. Opt.* **1998**, *37*, 170−180.

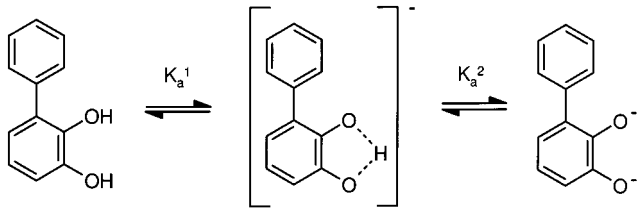

Figure 1. The protonation states of DHB. Based on a titration curve, pK_a^1 is 9.40 ± 0.05 in aqueous buffer. DHB was observed as a monoanion in 0.5% NaOH (~pH 13), as mixture of mono- and dianions in 10% NaOH (~pH 14), and as a dianion in 250 mM *tert*-butoxide/*tert*-butyl alcohol.

to the model. In subsequent steps, the model was improved by the addition or deletion of water molecules bound at other sites, the addition of one residue (Arg289) to the polypeptide chain, and the modeling of second conformations for 18 residues. Fe−ligand bond distances were harmonically restrained to an equilibrium distance of 2.2 Å using a weak force constant of 10 kcal·mol^{-1}·Å^{-2}. Bond length, bond angle, and planarity restraints similar to those used for aromatic side chains were applied to DHB, but the torsion angle between the rings was unrestrained. Figures 8 and 9 were prepared with the programs Molscript[45] and Raster3D.[46]

Results and Analysis

DHB and catechol, particularly in their monoanionic and dianionic forms, were O_2-labile. Exposure of catecholic solutions to air caused a rapid change in their color followed by the formation of a precipitate, most probably corresponding to the formation of quinones and their subsequent polymerization.[47] The O_2-lability of the catechols, even in the absence of DHBD, required all measurements to be made under strictly anaerobic conditions as described in the Experimental Section. Obviously, the ES samples were deprived of O_2 to prevent catalytic turnover.

The pK_a Values of DHB and Catechol. DHB and catechol can exist in three different formal charge states depending on the ionization state of the two hydroxyl groups of the catechol moiety (Figure 1). For both catechol and DHB, the first pK_a was 9.40 ± 0.05, in good agreement with the published value of 9.45 for catechol.[48] The pK_a for removal of the second proton from either compound could not be determined from titration data in aqueous solution. The second pK_a values of these 1,2-diols are higher than the second pK_a values of 1,3-dihydroxybenzene and 1,4-dihydroxybenzene (~11.0−11.4),[48] presumably due to the intramolecular hydrogen bond between the remaining oxygen-bound proton and the neighboring ionized oxygen atom.[49,50]

UV/Vis absorption spectroscopy and UVRRS were used to identify the predominant forms of DHB and catechol in 0.5% NaOH (~pH 13), 10% NaOH (~pH 14), methanol containing an excess of sodium methoxide (pK_a = 15.54)[51] and in *tert*-butyl alcohol containing an excess of sodium *t*-butoxide (pK_a = 18.00).[51] Spectra of the monoanionic and neutral species were measured in both normal and deuterated solvents to characterize the isotope induced shifts from the exchangeable hydroxyl protons and to compare with the data measured in the high pH solutions and nonaqueous solvents.

The UVRR and UV/Vis absorption spectra of DHB in 0.5% NaOH are essentially identical to those in pH 11 buffer solution, consistent with the presence of the monoanionic species alone. In contrast, the UVRR spectrum, recorded using 10% NaOH solution, showed components of the monoanionic species, which shift in a deuterated solution, and components of the presumed dianionic species, which do not. The two species were present at similar concentrations, indicating that the pK_a^2 of DHB is approximately 14. Interestingly, the UVRR spectrum and the observation of the same isotope-induced shifts observed in pH/pD 11 buffer indicated that DHB was predominantly monoanionic in a solution of methanol containing an excess of sodium methoxide (pK_a = 15.54), and thus that the pK_a^2 of DHB is higher in the lower dielectric solvent. However, a solution of DHB in *tert*-butyl alcohol containing an excess of sodium *tert*-butoxide (pK_a = 18.00) produced a new UVRR spectrum that was unchanged in *tert*-butyl alcohol-OD, as expected for the dianionic species. These two latter spectra could be used as components to exactly reproduce the spectrum of the mixture observed in the 10% NaOH aqueous solution.

The analogous spectra of catechol were also recorded and produced similar results. The lack of an isotope-induced shift in the UVRR spectrum of catechol in *tert*-butyl alcohol/*tert*-butoxide solution is indicative of dianionic species under these conditions while a different spectral signature in methanol/methoxide that produces several, albeit subtle, band shifts in the deuterated solution suggest the monoanionic species. The spectrum of the neutral catechol species was also measured and is in good agreement with published nonresonance Raman data.[52] The spectrum of catechol in 0.5% NaOH solution showed a superposition of the monoanionic and dianionic spectral features, consistent with the published pK_a^2 of catechol (13.3).[48] As in the case of DHB, these data indicate that the pK_a^2 of catechol is higher in the lower dielectric solvent. This is consistent with the observation that the pK_a^2 of catechol increases with methanol concentration.[53]

UV/Vis Absorption Spectroscopy of DHB and Catechol. The electronic absorption spectra of biphenyl and catechol were recorded to provide a basis for assigning the transitions in DHB and to interpret the spectrum of the ES complex. Spectra of biphenyl and the neutral species of catechol and DHB are compared in Figure 2A. The assigned maxima at the shortest wavelengths (<210 nm) are to be regarded with caution due to the high background absorption of the solvent in this region.

Deprotonation of the hydroxyl groups of DHB induced dramatic changes in the absorption spectrum (Figure 2B). In general, the removal of each proton resulted in successive red shifts of the lowest lying transitions and an increase in the extinction coefficients. The most obvious changes occur in the shift of the lowest energy transition from 283 nm for the neutral species in aqueous solution (pH 8) to 305 nm for the monoanionic species (pH 11) and to 348 nm for the dianionic species in *tert*-butyl alcohol/*tert*-butoxide. The next lowest transition

(45) Kraulis, P. J. *J. Appl. Crystallogr.* **1991**, *24*, 946−950.
(46) Merritt, E. A.; Bacon, D. J. *Methods Enzymol.* **1997**, *277*, 505−524.
(47) Raff, R.; Ettling, B. V. In *Encyclopedia of Chemical Technology*, 2nd ed.; Standen, A., Mark, H. F., McKetta. J. J., Jr., Othmer D. F., Eds.; Interscience: New York, 1963−1970; Vol. 11, pp 462−492.
(48) Smith, R. H.; Martell, A. E. *Critical Stability Constants (second supplement and earlier volumes)*; Plenum Press: New York, 1989.
(49) Gerhards, M.; Perl, W.; Schumm, S.; Henrichs, U.; Jacoby, C.; Kleinermanns, K. *J. Chem. Phys.* **1996**, *104*, 9362−9375.
(50) Ramirez, F. J.; Lopez-Navarrete, J. T. *J. Mol. Struct.* **1993**, *293*, 59−62.
(51) McMurry, J. *Organic Chemistry*; 3rd ed.; Brooks/Cole: Pacific Grove, CA, 1992.
(52) Lopez-Navarrete, J. T.; Ramirez, F. J. *Spectrochim. Acta, Part A* **1993**, *49A*, 1759−1767.
(53) Tyson, C. A.; Martell, A. E. *J. Am. Chem. Soc.* **1968**, *90*, 3379−3386.

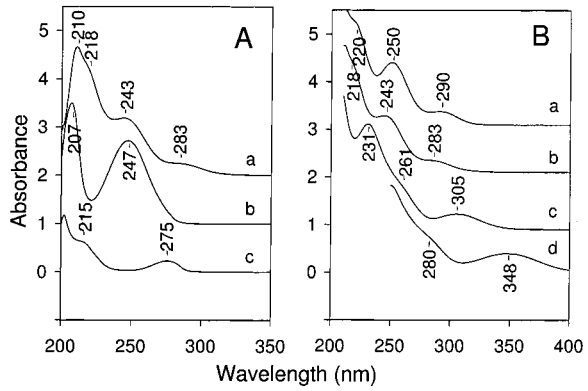

Figure 2. Electronic absorption spectra of DHB, biphenyl and catechol. Panel A depicts: (a) 100 μM DHB in 20 mM Tris pH 8.0; (b) 100 μM biphenyl in methanol; and (c) 100 μM catechol in 20 mM Tris pH 8.0. Panel B depicts: (a) 100 μM neutral DHB in *tert*-butyl alcohol; (b) 100 μM neutral DHB in 20 mM Tris pH 8.0; (c) 100 μM monoanionic DHB in potassium phosphate buffer pH 11 ($I = 0.1$); and (d) 100 μM dianionic DHB in 250 mM sodium *tert*-butoxide/*tert*-butyl alcohol solution. For clarity, each spectrum was offset by one absorbance unit with respect to the one below.

undergoes a similar red shift from 243 in the neutral species to 261 and 280 nm in the monoanion and dianion, respectively. The same pattern of decreased energy and increased intensity was observed in the transitions of catechol as each hydroxyl proton was removed (Table 1). The band maxima and extinction coefficients for each of the three species of both catechol and DHB, as well as the biphenyl transitions, are given in Table 1. Note that impurities in the *tert*-butoxide absorbed at the shorter wavelengths, limiting the reliable measurement of the dianionic catechols to wavelengths longer than approximately 245 nm.

UV/Vis Absorption Assignments via the Composite Molecule Model. A qualitative description of the electronic structure of DHB is useful for discussing the changes that occur upon removal of one or both hydroxyl protons. The spectrum of DHB can be approximated by the superposition of the spectra of catechol and biphenyl; additional features and variations are then understood in terms of the interaction of the benzene and catechol subsystems. This composite molecule model has been successfully applied to biphenyl[54,55] in which the two subsystems are simply two benzene molecules. As biphenyl is a convenient example from which to extend the model to the current system, a brief overview is given. For a complete discussion of the electronic structure of biphenyl, see Rubio et al.[55]

The first three allowed (singlet) excited states of benzene have symmetry of B_{2u}, B_{1u}, and E_{1u} in order of increasing energy and are, respectively, labeled L_b, L_a, and $B_{a,b}$ according to the notation of Platt.[56] This notation allows one to discuss transitions of the same nature in related aromatic molecules regardless of the changes in formal symmetry. In benzene, only the transition to $B_{a,b}$ from the ground state is allowed by strict symmetry selection rules. However, the other transitions are observed through vibronic interactions, albeit at much lower intensities. In a zeroth-order approximation of biphenyl, the two benzene subsystems do not interact at all, and the spectrum of the composite molecule is simply the superposition of its components, resulting in at least doubly degenerate excited states. This is, of course, not the case, as interaction between the two rings splits the degenerate levels. These interactions arise from the coupling of transition dipole moments in which the magnitude of the splitting is related to the strength and orientation of the interacting transition dipoles.[54,57] Interactions due to charge transfer between the two rings can be neglected because the energy of the charge-transfer transitions is far from the lowest lying excitations considered here.[58]

The maxima for biphenyl in solution at 207 and 247 nm have been assigned to the $B_{a,b}$ and the L_a transitions, respectively (Table 1).[54,55,59] The L_b transition is very weak and hidden under the long wavelength tail of the stronger L_a transition. However, two-photon excitation spectra in ethanol place the L_b transition at approximately 262 nm.[54] In the case of catechol, which has lower symmetry than planar biphenyl, both the L_a and L_b transitions are allowed and are consequently much stronger. Accordingly, the maxima observed for catechol at ~200, 215, and 275 nm are assigned to the B_{ab}, L_a, and L_b transitions, respectively. The L_a transition is close to that observed in benzene whereas the L_b transition occurs at a longer wavelength than in either benzene or biphenyl.

The interaction of the catechol and phenyl groups in DHB apparently produces splittings in the $B_{a,b}$ and L_a transitions similar to those of biphenyl, although the density of states and the lower symmetry of DHB compared to biphenyl precludes the assignment of more than the two lowest transitions with the current data. In the framework of the composite molecule model, the L_b transitions of the benzene components of biphenyl are not expected to be greatly perturbed because of the small transition dipole moment of the parent L_b transition in benzene. However, the two hydroxyl groups of the catechol component of DHB lead to a stronger transition dipole moment for the parent L_b transition, which should increase interaction and thus shift the resulting band in DHB to even lower energy. Accordingly, the bands at 243 and 283 nm were assigned to the L_a and L_b transitions, respectively, in DHB.

Solvent-Induced UV/Vis Absorption Spectral Changes. The absorption spectrum of DHB in a given ionization state was unaffected by the identity of the buffer in aqueous solutions (phosphate, CAPS, or Tris) or the use of deuterated solvents. However, the spectra of neutral and monoanionic DHB differed in aqueous and alcoholic solutions. The low-lying transitions of neutral DHB in *tert*-butyl alcohol (Figure 2B, spectrum a) or methanol were red-shifted from that in aqueous solution at pH 8.0 (Figure 2B, spectrum b). Solvent-induced band shifts of similar magnitude were observed for monoanionic DHB (i.e., a 7 nm red shift of the L_b transition in methanol/methoxide vs aqueous solution). Similar shifts in the electronic transitions of biphenyl have been attributed to the twist angle.[55,60] The L_a transition of biphenyl shifts to shorter wavelengths as the aromatic rings of the biphenyl molecule twist away from coplanarity. It is therefore concluded that DHB is more planar in *tert*-butyl alcohol and methanol than in water, regardless of its ionization state. Consistent with this reasoning, there were

(54) Dick, B.; Hohlneicher, G. *Chem. Phys.* **1985**, *94*, 131−145.
(55) Rubio, M.; Merchan, M.; Orti, E.; Roos, B. O. *Chem. Phys. Lett.* **1995**, *234*, 373−381.
(56) Platt, J. R. *J. Chem. Phys.* **1949**, *17*, 484−495.
(57) Swiderek, P.; Michaud, M.; Hohlneicher, G.; Sanche, L. *Chem. Phys. Lett.* **1991**, *187*, 583−589.
(58) Suzuki, H. *Electronic absorption spectra, and geometry of organic molecules; an application of molecular orbital theory*; Academic Press: New York, 1967.
(59) Sett, P.; Chattopadhyay, S.; Mallick, P. K. *Chem. Phys. Lett.* **2000**, *331*, 215−223.
(60) Suzuki, H. *Bull. Chem. Soc. Jpn.* **1959**, *32*, 1347.

Table 1. Electronic Absorption Bands of Catechol, Biphenyl, and DHB[a]

assignment[b]	catechol (nm (M^{-1} cm^{-1}))	catechol$^-$ (nm (M^{-1} cm^{-1}))	catechol^{2-} (nm (M^{-1} cm^{-1}))	biphenyl (nm (M^{-1} cm^{-1}))	DHB (nm (M^{-1} cm^{-1}))	DHB$^-$ (nm (M^{-1} cm^{-1}))	DHB^{2-} (nm (M^{-1} cm^{-1}))	bound DHB (nm (M^{-1} cm^{-1}))
$B_{a,b}$	<200 (<16000)	<220	<240	207 (24900)	~210 (>30000) 218 (22700)	<206 231 (22100)	<250	
L_a	215 (6300)	237 (7700)	256 (8700)	247 (17200)	243 (11800)	261 (8700)	280 (8000)	~261 (6000)
L_b	275 (2300)	289 (4300)	308 (7600)	262[c]	283 (2500)	305 (3200)	348 (4000)	299 (2300)

[a] The spectra of catechol and DHB were taken in 20 mM Tris pH 8.0. The spectra of catechol$^-$ and DHB$^-$ were taken in potassium phosphate buffer pH 11 ($I = 0.1$). The spectra of catechol^{2-} and DHB^{2-} were taken in 250 mM sodium *tert*-butoxide/*tert*-butyl alcohol solution, and the spectrum of biphenyl was recorded in methanol. Values in parentheses represent extinction coefficients in M^{-1} cm^{-1}. [b] Notation according to Platt.[56] [c] Taken from two-photon absorption data.[54]

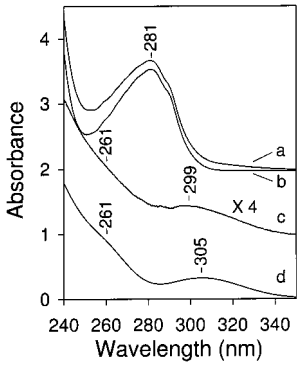

Figure 3. Electronic absorption spectra of DHBD-bound DHB. (a) Spectrum of 43 μM DHBD with 25 μM DHB (20 mM Tris pH 8.0, 25 °C). (b) Spectrum of 43 μM DHBD (20 mM Tris pH 8.0, 25 °C). (c) Difference spectrum (a − b). (d) Spectrum of 100 μM monoanionic DHB (potassium phosphate buffer pH 11 ($I = 0.1$), 25 °C). For clarity, spectra a and b were overlaid and the others were offset by one absorbance unit with respect to the one below it.

no significant solvent-induced shifts in the transitions of catechol (data not shown). Finally, it is noted that while the solvent-induced shifts in the DHB transitions are significant and easily measurable, their magnitude is not sufficient to explain those induced by deprotonation, which shift the L_b transition by up to 40 nm.

UV/Vis Absorption of DHBD-Bound DHB. The spectrum of DHBD:DHB is dominated by absorption due to peptide bonds and aromatic residues of the enzyme. Thus, the spectrum of bound DHB was obtained by subtracting the spectrum of DHBD from that of the DHBD:DHB complex (Figure 3) for wavelengths longer than 240 nm. It is possible that substrate-induced changes in the environment of Tyr250 (vide infra) might affect the spectrum of DHBD. However, the difference spectrum clearly reveals a significant band with a maximum at 299 nm ($\epsilon \sim 2300$ M^{-1} cm^{-1}; Table 1), which is assigned to the lowest transition of bound DHB through comparison with spectra of free DHB. Addition of DHB to a concentration twice that of the enzyme concentration resulted in an absorption peak corresponding to neutral DHB in buffer superimposed upon the spectrum of the bound species (data not shown).

The maximum for the lowest transition of DHBD-bound DHB is most similar to that of monoanionic DHB in aqueous solution (305 nm), indicating that the bound substrate is monoanionic. Moreover, the 6 nm blue shift of the L_b transition of bound DHB with respect to that of monoanionic DHB in aqueous solution suggests that the twist angle of DHB increases upon binding to the enzyme. While this conclusion is consistent with the structural data, which show that the two rings of DHB are orthogonal to within 6° in the ES complex (vide infra), it is also possible that the blue shift reflects the binding of the catechol to the iron and/or the hydrogen bonding of the catechol in the enzyme's active site.

UVRRS. The resonance Raman spectra of DHB are expected to derive mainly from delocalized ring vibrations[61] but will be significantly affected by the ionization state inasmuch as certain modes will contain or be coupled to motions of the hydroxyl groups. The Raman spectra will therefore also be affected by the isotopic substitution of the exchangeable protons on the hydroxyl groups, which provides a means to positively identify the dianionic species of DHB from the absence of an isotopically induced vibrational shift in the Raman spectrum measured in deuterated solvents. Conversely, the observation of such a shift in the vibrational frequencies of DHB in deuterated solvent can only arise from the replacement of one or both hydroxyl protons by deuterons. One of the reasons for employing UVRRS was to take advantage of higher sensitivity and selectivity through resonance. By tuning the wavelength of excitation to be in resonance with an electronic transition of DHB, it was anticipated that the spectrum of the bound DHB would be selectively enhanced over the expected competing signals of the protein and solvent. This approach was constrained however, by the availability of suitable wavelengths from the laser and the characteristics of the complex under study. At shorter accessible wavelengths, such as 229.2 nm, the aromatic amino acid residues dominate the spectrum due to their relatively high number and large Raman scattering cross-section. In contrast, at the longest available wavelength (257.2 nm), where the cross-section of DHB relative to the aromatic amino acid residues is most favorable, the Raman signal is overwhelmed by fluorescence, primarily from the phenylalanine and tyrosine residues.[62]

A measurement of the resonance enhancement profile (Figure 4) of free, neutral DHB in aqueous solution showed that the 248.2 nm line from the laser was the most appropriate wavelength for maximizing the signal of DHB relative to the protein while avoiding the fluorescence. The strongest bands of neutral DHB are more enhanced at the shortest wavelengths, but are approximately 1 order of magnitude weaker than the aromatic amino acid bands.[63,64] However, the red shift in the absorption spectrum of the DHBD-bound DHB brings it into better resonance at 248.2 nm. Furthermore, the most important marker for detecting the isotope induced shift is a medium strength band at ca. 1300 cm^{-1}, which is clearly coupled to the lower energy L_b transition. The 248.2 nm line was chosen

(61) Varsanyi, G. *Vibrational Spectra of Benzene Derivatives*; Academic Press: New York, 1969.
(62) Wen, Z. Q.; Thomas, G. J. *Biopolymers* **1998**, *45*, 247−256.
(63) Austin, J. C.; Jordan, T.; Spiro, T. G. In *Biomolecular Spectroscopy, Part A*; Clark, R. J. H., Hester, R. E., Eds.; John Wiley & Sons: Chichester, England, 1993; Vol. 20, pp 55−126.
(64) Wen, Z. Q.; Armstrong, A.; Thomas, G. J. *Biochemistry* **1999**, *38*, 3148−3156.

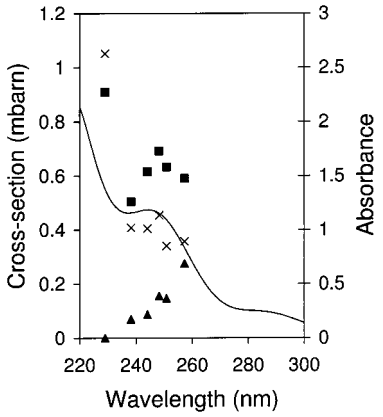

Figure 4. Resonance Raman enhancement profile of selected DHB bands. Cross-sections for the bands at 1614 cm^{-1} (x), 1605 cm^{-1} (■) and 1304 cm^{-1} (▲) were measured at the wavelengths available from a frequency-doubled argon ion laser relative to the signal from perchlorate present in solution as an internal standard. The absorption spectrum of 100 μM DHB (20 mM Tris, pH 8.0; Figure 2A, spectrum a) is overlaid on a secondary axis to illustrate the resonant enhancement of the vibrations with the particular electronic transition(s).

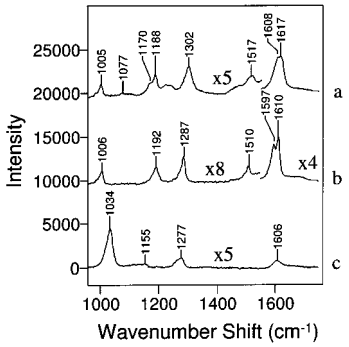

Figure 5. UVRR spectra of DHB, biphenyl and catechol. (a) 2 mM neutral DHB in methanol (4 min). (b) 2 mM biphenyl in methanol (2 min). (c) 20 mM neutral catechol in methanol (3 min). The data shown were averaged over a number of 10 s acquisitions using 20 mW of 248.2 nm excitation. Total integration times are indicated in parentheses.

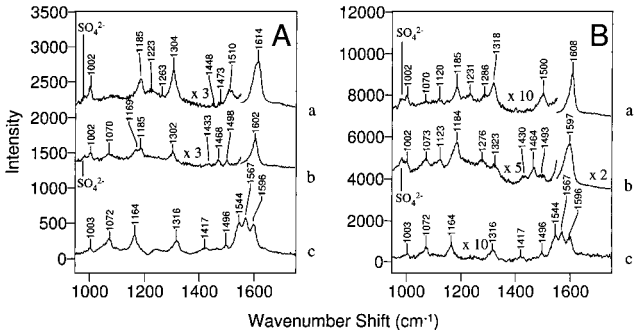

Figure 6. UVRR spectra of free DHB in protonated (A) and deuterated (B) solvents. Panel A depicts: (a) 2 mM neutral DHB in 20 mM Tris pH 8.0, 100 mM Na_2SO_4 (4.5 min); (b) 2 mM monoanionic DHB in potassium phosphate buffer pH 11 ($I = 0.1$), 100 mM Na_2SO_4 (6 min); and (c) 2 mM dianionic DHB in 250 mM sodium *tert*-butoxide/*tert*-butyl alcohol solution (1.5 min). Panel B depicts: (a) 2 mM neutral DHB in deuterated 20 mM Tris pD 8.0, 100 mM Na_2SO_4 (4.5 min); (b) 2 mM monoanionic DHB in deuterated potassium phosphate buffer pD 11 ($I = 0.1$), 100 mM Na_2SO_4 (0.5 min); and (c) 2 mM dianionic DHB in 250 mM sodium *tert*-butoxide/*tert*-butyl alcohol-OD solution (2 min). The data shown were averaged over a number of 10 s acquisitions using 20 mW of 248.2 nm excitation. Total integration times are indicated in parentheses.

instead of the 251 nm line because more power was available and because no significant differences were observed in the cross-section or absorption properties of the sample that would affect collection efficiency of the fiber-optic probe.[43,44]

As with the absorption spectra, resonance Raman spectra were recorded for DHB in at least two different solvents for the neutral and monoanionic forms to determine whether the nonaqueous solvent necessary for generating the dianion induces spectral changes. In addition to inducing changes in the twist angle, the solvent may induce changes in the relative positions of the hydroxyl protons due to different hydrogen-bonding environments. In catechol, such changes cause small band shifts and polarization changes of certain nontotally symmetric vibrations.[50,52] However, the spectra of the DHB species were not significantly affected by solvent, indicating that the most prominent bands observed with 248.2 nm excitation are relatively insensitive to the twist angle of the phenyl rings and the hydrogen-bonding environment of the hydroxyl groups. Finally, as a precautionary measure, a small amount of sodium hydrosulfite was added to the DHBD:DHB samples to prevent turnover by the enzyme, which could be detected by the appearance of the yellow product and characteristic changes in the Raman spectra. Hydrosulfite had no effect on the spectra of DHB at concentrations up to 2 mM. However, as this compound absorbs significantly at 248.2 nm, the excitation wavelength used in this study, its concentration was minimized to optimize the signal-to-noise ratio.

UVRRS of DHB in Solution. The UVRR spectra of DHB were compared to those of biphenyl and catechol to provide a basis for assigning the observed transitions and to interpret the spectrum of the DHBD-bound DHB. As shown in Figure 5, the spectrum of the neutral species of DHB in methanol more closely resembles that of biphenyl than that of neutral catechol.

The Raman spectra of the three ionization states of DHB revealed that deprotonation of the neutral species (Figure 6A, spectrum a) to the monoanion (Figure 6A, spectrum b) caused the following changes: a shift of the 1614/1605 cm^{-1} doublet accompanied by the reduction in the low wavenumber component; the appearance of three weak bands from 1500 to ~1400 cm^{-1} with concomitant loss of the prominent band at 1510 cm^{-1}; a shift of the 1304 cm^{-1} band to 1302 cm^{-1}; the appearance of a Fermi doublet at 1185/1169 cm^{-1} which replaces the 1185 cm^{-1} fundamental; and the replacement of two weak and unresolved features centered at ~1085 cm^{-1} by a band at 1070 cm^{-1}. Further deprotonation of DHB to the dianion induces more dramatic changes in the spectrum (Figure 6A, spectrum c) including the replacement of the ca. 1602 cm^{-1} doublet as the strongest feature by three moderately resolved, strong bands at 1596, 1567 and 1544 cm^{-1}, the replacement of the three weak bands from 1500 to 1442 cm^{-1} by bands at 1496, 1448, 1427, and 1417 cm^{-1}, the upshifting of the 1300 cm^{-1} feature to 1316 cm^{-1}, loss of the Fermi resonance at 1185/1169 cm^{-1} leaving the fundamental shifted down to 1164 cm^{-1}, and an increase in intensity of the band at 1072 cm^{-1}. A feature at 1002 cm^{-1} remains essentially constant throughout this series, although it is measured at 1003 cm^{-1} in the spectrum of the dianionic species.

The spectrum of DHB in *tert*-butoxide/*tert*-butyl alcohol-OD solution (Figure 6B, spectrum c) is essentially identical to that recorded in *tert*-butoxide/*tert*-butyl alcohol solution. This is consistent with the expected absence of exchangeable protons in the dianionic form of DHB. In contrast, the spectra of

Table 2. Resonance Raman Bands of DHB at 248.2 nm Excitation[a]

DHB		DHB^-			bound DHB			
h_2 (cm^{-1})	d_2 (cm^{-1})	h_1 (cm^{-1})	d_1 (cm^{-1})	DHB^{2-} (cm^{-1})	H (cm^{-1})	D (cm^{-1})	biphenyl (cm^{-1})	assignment[b]
1614 (s)	1608 (s)	1602 (s)	1597 (s)	1596 (s)	1603 (s)	1603 (s)	1610 (s)	A_g 4
1605 (s)	~1590 (sh)	~1590 (sh)	~1580 (sh)	1567 (s)			1597 (s)	B_{3u} 4
1510 (m)	1500 (m)	1498 (m)	~1493 (w)	1544 (s)	1504 (w)	1490 (bw)	1510 (m)	A_g 5
~1473 (vw)	1472 (w)	1468 (m)	1464 (m)	1496 (m)	~1467 (vw)	1453 (w)	1452 (w)	B_{1g} 4
1448 (w)		1433 (m)	~1430 (w)	1427 (m)				B_{2u} 4
	1399 (w)		1375 (w)	1417 (m)				
1304 (m)	1318 (m)	1302 (m)	1323 (m)	1316 (m)	1306 (m)	1316 (m)		B_{1g} 6
~1263 (vw)	1286 (w)	~1245 (vw)	1276 (m)	1244 (bw)	1262 (w)	~1282 (sh)	1287 (m)	A_g 6
~1223 (bw)	1231 (w)	~1218 (vw)			1227 (w)			B_{2u} 6
1185 (m)	1185 (m)	1185 (m)	1184 (m)	1164 (m)	1175 (m)	1173 (m)	1192 (m)	A_g 7
		1169 (m)			1186 (m)	1192 (w)		$2 \times B_{2g}$ 4
~1096 (bw)	~1120 (bw)	~1107 (sh)	1123 (m)	~1100 (vw)	1093 (w)	~1106 (w)		B_{1g} 8
~1077 (bw)	~1070 (bw)	1070 (m)	1073 (m)	1072 (m)	1062 (w)	~1050 (w)		B_{2u} 8
~1051 (w)		~1050 (sh)		~1048 (sh)	~1033 (vw)			
1002 (m)	1002 (m)	1002 (m)	1002 (m)	1003 (m)	1002 (w)	1002 (w)	1006 (m)	A_g 9

[a] The letters in parentheses represent the intensity and shape of the Raman band according to the following letter code: strong (s), medium (m), weak (w), very weak (vw), broad (b), shoulder (sh). [b] Assignment based on biphenyl according to Zerbi and Sandroni.[65,66]

monoanionic and neutral DHB were affected by deuterated solvents due to exchange of the hydroxyl proton(s) for deuteron(s). The spectrum of monoanionic DHB in deuterated buffer (Figure 6B, spectrum b) differs from that in protonated buffer in the following respects: a slight broadening of the strongest band and its shift to 1597 cm^{-1}; a 21 cm^{-1} upshift of the 1302 cm^{-1} band; a shift and increase in intensity of the very weak feature at ~1245 cm^{-1} to 1276 cm^{-1}; loss of the Fermi resonance leaving only the fundamental at 1184 cm^{-1}; and a new feature at 1123 cm^{-1}. The spectrum of neutral DHB in deuterated buffer (Figure 6B, spectrum a) differs from that in protonated buffer in the following respects: a downshift of the strongest feature to 1608/1590 cm^{-1} with a reduction in intensity of the low wavenumber component; a downshift of the 1510 cm^{-1} band to 1500 cm^{-1}; upshifts of bands at 1304,~1263, and ~1223 cm^{-1} to 1318, 1286, and 1231 cm^{-1}, respectively. The bands at 1185 and 1002 cm^{-1} are not affected by the H/D exchange. While band shifts to higher frequencies upon H/D exchange may seem counterintuitive, recent theoretical calculations on catechol predict shifts consistent with those observed for DHB for a number of vibrations.[49]

UVRRS Spectral Assignments. Band assignments for DHB based on the similarity of structure and spectrum to biphenyl are proposed in Table 2. The vibrational modes are labeled according to biphenyl vibrations as described by Zerbi and Sandroni.[65,66] The vibrational spectrum of biphenyl has been well characterized[65,67−69] and, except for one band deriving from a B_{1u} vibration in planar biphenyl, only the totally symmetric vibrations, derived from A_g vibrations, are significantly enhanced at 248.2 nm of excitation. The profile of the stronger bands in the spectrum of neutral DHB corresponds to that of biphenyl, allowing facile assignment of these bands. The weaker bands in the DHB spectrum correlate well with biphenyl vibrations observed under nonresonance conditions. This is consistent with formal symmetry selection rules that are applicable to the biphenyl molecule but are relaxed because of the lower symmetry of DHB.

The similarity of the spectra of monoanionic and neutral DHB enables the assignment of the monoanion's bands through comparison. The markedly different spectrum of dianionic DHB, with respect to both the intensity and vibrational frequency of the bands, hinders such a straightforward assignment. This difference is due to the large change in the electronic structure of dianionic DHB described in the UV/Vis absorption section. The shifts of the low lying electronic states are such that at the wavelength of excitation, the dianion is resonant with a different electronic state than the neutral or monoanionic species.

UVRRS of DHB Bound to DHBD. A major concern in experiments involving DHBD was the sensitivity of the sample to the UV radiation of the laser. To address this issue, the stability of the protein was investigated using various power levels and exposure times. The final experimental protocol included the removal of aliquots of sample after each exposure to the laser, and sample integrity was verified according to the specific activity of the protein. Samples exposed to 20 mW of 248.2 nm light from the laser for 10 s retained a minimum of 85% of their initial activity.

The spectrum of the ES complex was dominated by signal from the aromatic amino acids despite attempts to selectively enhance the bound substrate signal through judicious choice of wavelength (Figure 7). This background of protein signal was up to one order of magnitude stronger than the underlying DHB signal and necessitated careful spectral subtraction to extract the data of interest. The 982 cm^{-1} peak of sulfate was used to normalize the intensities. No absorption correction was made across the spectral window as the correction term was found to be negligible. This is because the absorption properties of the sample are dominated by the protein, which is common to both parent spectra (i.e., DHB did not significantly affect the absorption properties of the protein solution). Finally, the close resemblance of the difference spectrum to that of DHB indicates that this spectrum does not contain a significant contribution from the protein. This could have been the case, particularly if the environment of one or more aromatic amino acid residues changes significantly upon DHB-binding.[32,70−73]

(65) Zerbi, G.; Sandroni, S. *Spectrochim. Acta, Part A* **1968**, *24A*, 511−528.
(66) Zerbi, G.; Sandroni, S. *Spectrochim. Acta, Part A* **1968**, *24A*, 483−510.
(67) Almenningen, A.; Bastiansen, O.; Fernholt, L.; Cyvin, B. N.; Cyvin, S. J.; Samdal, S. *J. Mol. Struct.* **1985**, *128*, 59−76.
(68) Barrett, R. M.; Steele, D. *J. Mol. Struct.* **1972**, *11*, 105−125.
(69) Sasaki, Y.; Hamaguchi, H.-O. *Spectrochim. Acta, Part A* **1994**, *50A*, 1475−1485.
(70) Lednev, I. K.; Karnoup, A. S.; Sparrow, M. C.; Asher, S. A. *J. Am. Chem. Soc.* **1999**, *121*, 8074−8086.
(71) Chi, Z. H.; Asher, S. A. *J. Phys. Chem.* **1998**, *102*, 2B, 9595−9602.
(72) Hu, X. H.; Spiro, T. G. *Biochemistry* **1997**, *36*, 15701−15712.
(73) Jordan, T.; Eads, J. C.; Spiro, T. G. *Protein Sci.* **1995**, *4*, 716−728.

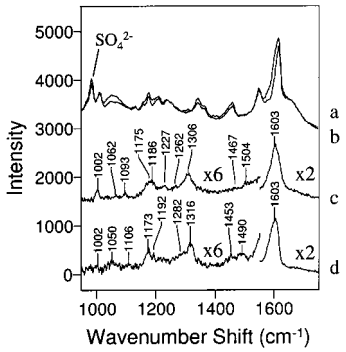

Figure 7. UVRR spectra of DHBD-bound DHB. (a) Spectrum of 140 μM DHBD with 110 μM DHB (20 mM Tris pH 8.0, 100 mM Na_2SO_4; 10 μM $Na_2S_2O_4$; 100 s). (b) Spectrum of 140 μM DHBD (20 mM Tris pH 8.0, 100 mM Na_2SO_4; 10 μM $Na_2S_2O_4$; 70 s) overlaid on the same scale as spectrum a. (c) Difference spectrum showing 110 μM bound DHB in protonated solvent (100 s). (d) Difference spectrum showing 103 μM bound DHB in deuterated solvent (130 s). The data shown are spectra averaged over a number of 10 s acquisitions with 20 mW of 248.2 nm excitation. Total integration times are indicated in parentheses (i.e., number of spectra averaged = total integration time/10 s). The absence of the internal standard SO_4^{2-} signal in the difference spectra indicates proper subtraction of the parent spectra.

The resonance Raman spectrum of DHBD-bound DHB in aqueous solution, obtained by subtracting the spectrum of DHBD from that of DHBD:DHB complex, is shown in Figure 7 for H_2O (spectrum c) and D_2O (spectrum d) solution. The strongest feature occurred at 1603 cm^{-1}, which coincides with a feature in the spectrum of monoanionic DHB in H_2O (Figure 6) and is 11 cm^{-1} below that of the corresponding feature in neutral DHB. The distinctive spectrum of dianionic DHB in the 1600 cm^{-1} region (Figure 6) is not observed in the spectrum of DHBD-bound DHB. The remaining weak bands in the difference spectrum do not clearly distinguish between neutral and monoanionic DHB, but the position of the 1603 cm^{-1} band identifies the bound substrate as the monoanion.

Interestingly, D_2O did not affect the spectrum of bound DHB in the same manner as that of the free DHB monoanion. Thus, the strongest feature, which shifts from 1602 to 1597 cm^{-1} in the spectrum of the free monoanion (Figure 6), does not shift in the spectrum of the bound monoanion (Figure 7). However, D_2O induces a slight change in its shape, suggesting that it comprises more than one component. A clearer indication of H/D exchange in the bound substrate is the upshift of the medium strength 1306 cm^{-1} band to 1316 cm^{-1}. Other deuterium-induced differences in the spectrum of DHBD-bound DHB include the following: the shift of weak bands at ca.1504 and 1467 cm^{-1} shift to ca. 1490 and 1453 cm^{-1}, respectively; upshift of the 1262 cm^{-1} band to $\sim$1282 cm^{-1}; splitting of the 1186/1175 doublet such that the high-frequency component shifts to 1192 cm^{-1}; an upshift of the weak band at 1093 cm^{-1} to 1106 cm^{-1}; and a weakening of the 1002 cm^{-1} band.

The insensitivity of the 1603 cm^{-1} band to H/D exchange is probably due to the hydrogen-bonding of the enzyme-bound substrate. This band is a ring mode with some involvement of the O−H bending displacement, analogous to the well-known Y8a mode of tyrosine, which also shifts down a few cm^{-1} in D_2O.[74,75] This O−H bending is also responsible for the 5 cm^{-1} downshift of the 1602 cm^{-1} band in free DHB monoanion, and is evidently suppressed in the enzyme-bound monoanion. Examination of the crystal structure of the DHBD:DHB complex reveals that the carboxylate of Asp244 is indirectly linked to the 3-hydroxyl of the bound DHB (i.e., that hydroxyl group thought to be protonated based on the Fe-substrate distances (vide infra)) via a bridging solvent species. These interactions would hinder hydrogen-atom motion perpendicular to the O−H bond, and thereby suppress involvement of the O−H bending displacement in the 1603 cm^{-1} normal mode.

In summary, the UVRR data are consistent with the UV/Vis absorption spectra in that they identify the species as the monoanion, albeit with an interesting alteration in the effect of H/D exchange on the RR spectra of enzyme-bound DHB.

DHBD:DHB Crystal Structure. A model of the enzyme:DHB was refined to R and R_{free} values of 0.161 and 0.196 based on 26435 and 1663 reflections, respectively, between 7.0 and 2.0 Å.[11] The final model included residues 2−289 from the single monomer in the asymmetric unit, one Fe atom, one DHB molecule, one *tert*-butyl alcohol molecule, and 115 water oxygen atoms, for a total of 2352 unique atoms. 100 atoms from 18 protein residues were included at half occupancy in each of two conformations. The coordinates of the final model were deposited in the Protein Databank (1KMY). In a prior publication we discussed structural features of the complex related to the stabilization and inhibition of DHBD by *tert*-butyl alcohol.[11] Here we report additional structural data pertinent to the chemical mechanism.

Superposition of the substrate-free and enzyme:DHB Cα models produced an rms deviation of 0.15 Å for 287 atoms, whereas the result for residues 137−288 was 0.19 Å. The difference reflects changes induced by substrate binding, which occurs inside a funnel-shaped cavity that lies entirely within the C-terminal half of the monomer. The largest differences in backbone position are found in three segments that border the DHB binding site and contain residues in contact with bound DHB. Thus, for residues 175−183, 202−211, and 241−246, six or more contiguous Cα atoms are displaced by at least 0.2 Å, and the active site cavity widens along the long axis of DHB such that the distance between the Cα atoms of residues 210 and 244 increases from 15.0 to 15.8 Å. With respect to positions of side chain atoms, two specific changes are noteworthy. The first, as illustrated in Figure 8, is a concerted movement of the Fe and its protein ligands by 0.5−0.6 Å away from the closed end of the binding cavity (Asp244). This change helps to establish space for the substrate's catechol ring. A second rearrangement, which appears to be of mechanistic significance, involves the side chains of three strictly conserved residues:[4] His241, Tyr250, and Glu260. In the substrate-free enzyme, His241 is presumed to be in the imidazole (neutral) state because of its proximity to the Fe(II) atom and its hydrogen bonding interactions: atom Nδ1 acts as donor in a hydrogen bond with the carbonyl group of Pro280 and atom Nϵ1 serves as acceptor in a bond with Oη of Tyr250. In the enzyme:DHB complex, the side chains of His241 and Glu260 have rotated toward each other such that the separation between 241-Nϵ1 and 260-Oϵ2 is reduced from 3.4 to 2.7 Å. This change does not disrupt the hydrogen bond between Nδ1 and the carbonyl of Pro280, which implies that His241 has acquired a proton during formation of the ES complex. The distance between 250-Oη and 241-Nϵ1

(74) Takeuchi, H.; Watanabe, N.; Harada, I. *Spectrochim. Acta, Part A* **1988**, *44A*, 749−761.
(75) Okishio, N.; Fukuda, R.; Nagai, M.; Nagai, Y.; Nagatomo, S.; Kitagawa, T. *J. Raman Spectrosc.* **1998**, *29*, 31−39.

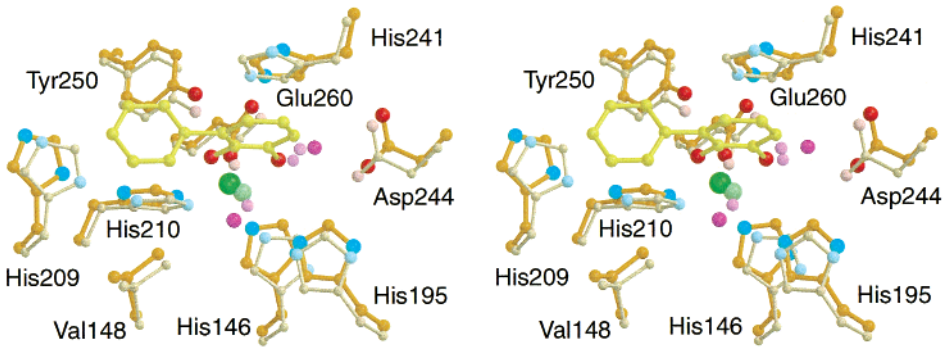

Figure 8. Displacements of active site atoms/residues associated with substrate binding. This is a (divergent) stereoscopic diagram. Atoms and bonds in the substrate-free structure are represented by smaller spheres, thinner sticks, and lighter shades. Carbon atoms are colored orange in protein residues and yellow in DHB. Nitrogen and iron atoms are cyan and green, respectively. Protein and DHB oxygen atoms are red, whereas water oxygens are magenta.

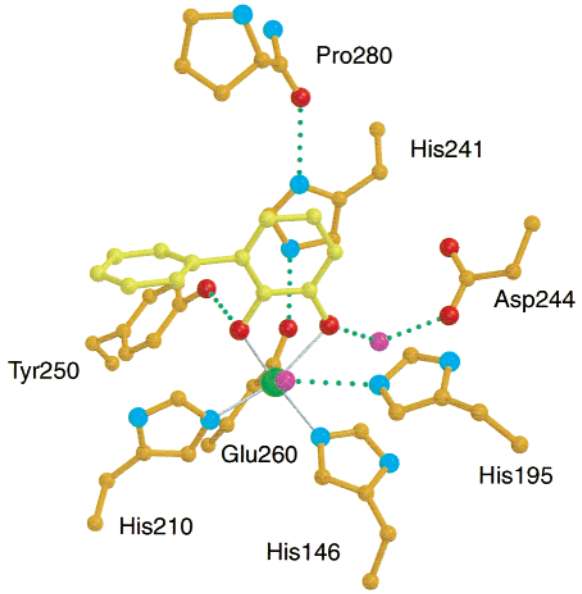

Figure 9. Hydrogen bonding in the active site of the DHBD:DHB complex. Carbon atoms are colored orange in protein residues and yellow in DHB. Oxygen, nitrogen, and iron atoms are colored red, cyan, and green, respectively. Fe−ligand bonds are indicated by gray sticks, and hydrogen bonds are indicated by green dotted lines.

Table 3. Fe−Ligand Distances and Ligand−Fe−Ligand Angles for the DHDB:DHB Complex[a]

Distances (Å)					
Fe−Nϵ2,His146	2.2	Fe−Nϵ2,His210	2.3	Fe−Oϵ1,Glu260	2.0
Fe−O2,DHB300	2.0	Fe−O3,DHB300	2.4	Fe−O,wat9003	2.4
Angles, deg					
146−Fe−210	99	146−Fe−260	103	146−Fe−O2	148
146−Fe−O3	97	146−Fe−9003	74	210−Fe−260	90
210−Fe−O2	85	210−Fe−O3	163	210−Fe−9003	163
260−Fe−O2	108	260−Fe−O3	94	260−Fe−9003	175
O2−Fe−O3	78	O2−Fe −9003	75	O3−Fe −9003	82

[a] For the angles, residue numbers 146, 210, 260, and 9003 correspond to the atoms defined by the distance specifications above. O2 and O3 refer to oxygen atoms of 2,3-dihydroxybiphenyl.

increases slightly (from 2.7 to 2.9 Å) and the 2-hydroxyl oxygen of the substrate replaces 241-Nϵ1 as the hydrogen bond acceptor closest to 250-Oη. A hydrogen bonding scheme consistent with the model is presented in Figure 9. Similar hydrogen bonding for the residues equivalent to His241 and Tyr250 was observed in a crystallographic study of a reactivated homologue, but no mechanistic significance was ascribed.[12]

Substrate binding also displaces ordered waters and a *tert*-butyl alcohol molecule. In the substrate-free structure, two waters are ligands to the Fe atom.[6] Both also associate with the protein through hydrogen bonds, in one case to Nϵ2 of His195, water 3012, and in the other to Oδ2 of Asp244, water 3001. A third water molecule, 4014, links both water ligands to Oδ1 of Asn243 through hydrogen bonds. Finally, a *tert*-butyl alcohol molecule binds with its central atom 6.0 Å from the Fe atom, but without a well-defined orientation, on a surface defined by several active site residues. As shown in Figure 8, DHB binding completely displaces waters 4014, and the *tert*-butyl alcohol molecule,[11] such that their locations are occupied by atom C4 of the catechol ring, and the distal ring of the substrate, respectively. Water 3001 is effectively displaced from the Fe by the substrate's 3-hydroxyl group. However, a change in the conformation of Met246 establishes a new binding site occupied by water 9002, which bridges between Asp244 and the 3-hydroxyl group. A similar arrangement is observed in the structure of a reactivated homologue.[12]

Substrate binding, and perhaps the movements of protein atoms, also apparently weaken the association between water 3012 and the Fe. A water remains in a position between His195 and the Fe, water 9001, but the Fe−water distance increases from 2.1 to 2.4 Å, whereas the distance to Nϵ2 of His195, 2.7 Å, does not change. This water site overlaps the likely site for dioxygen binding and is observed at lower apparent occupancies in structures obtained from crystals prepared by different protocols (data not shown). In contrast, this water site is not occupied in the structure of the enzyme:DHB complex of a reactivated homologue, and a hydrogen bond of length 3.1 Å is inferred between the substrates 3-hydroxyl and Nϵ2 of the equivalent His residue.[12] Such a hydrogen bond is less consistent with the structure reported here inasmuch as the corresponding distance is 3.5 Å and the donor−acceptor geometry is less appropriate. However, minor fluctuations in structure and loss of the water could allow such an interaction to form.

The coordination geometry in the substrate-free form of the enzyme is that of a well-defined square pyramid, with His146 as the axial ligand, and His210, Glu260, and the two waters in the basal plane.[6] Table 3 provides metric data that define the first coordination sphere in the enzyme:DHB complex. In this case, the geometric features allow only equivocal classification. One possible description is that of a distorted octahedron, with both the 3-OH group of the substrate and the water near His195 included as weak ligands. Prior crystallographic and spectroscopic studies of homologues[8,12] suggested a five-coordinate site

with the three protein side chains and the two hydroxyl groups of the substrate as ligands. For this ligand set, the geometry we observe is intermediate between square planar and trigonal bipyramidal, but strongly biased toward the former. This can be demonstrated by calculation of the parameter τ, which has been used in the context of inorganic complexes to characterize five-coordinate systems.[76] τ is defined by the equation $\tau = (\beta - \alpha)/60$, where β and α are the largest and second largest ligand−metal-ligand angles. For an ideal trigonal bipyramid $\tau = 1$, whereas $\tau = 0$ for a square pyramid. For the free-enzyme, $\tau = 0.05$, whereas $\tau = 0.25$ for the enzyme:DHB complex reported here, as compared to 0.27 for the DHB complex of a reactivated homologue.[12]

One face of the catechol ring stacks with His241 and the other is involved in five nonbonded contacts with side chains atoms Cϵ2 and Cζ2 of Phe187. His241 is fixed by hydrogen bonding, as described below, whereas Phe187 is pinned on the Cδ2,Cϵ2 edge by contacts with His195 and on the Cδ1,Cϵ1 edge by contacts with backbone atoms from two adjacent β strands. The C4−C5 edge of DHB is positioned by contacts with Asn243 and Ile173, whereas atom C6 is in contact with the side chain of Pro280. Thus the catechol ring binds in a restricted pocket that is highly complementary in size and shape.

In contrast, the space available for the phenyl ring of DHB appears to be substantially less restricted in that not one atom has multiple contacts at distances of 3.8 Å or less. The dihedral angle between the catechol and phenyl rings of bound DHB deviates from orthogonality by 6°, which seems to reflect contacts between CB2 and CB5 of the phenyl ring with Oη of Tyr250 and Cϵ2 of Phe202, respectively. In the enzyme:DHB structure of a reactivated homologue,[12] the dihedral angle deviates from orthogonality by 25°, and from the value reported here by 31°.

Discussion

This study establishes the utility of UVRRS as a probe of substrate binding in catechol-transforming enzymes, including ring-cleaving dioxygenases. Two factors were critical for success: rapid data acquisition and the selectivity achieved by resonant excitation. The former was critical due to the photolability of the enzyme. Short acquisition times (10 s) were achieved using a custom-designed fiber optic probe. The excitation wavelength was optimized to minimize interference from the large Raman scattering cross-section and fluorescence of aromatic amino acid residues. Deprotonation of the catecholic substrate, as postulated in ring-cleavage enzymes, actually increases the utility of UVRRS, as deprotonation red-shifts the electronic transitions to a window of wavelengths between 230 and 260 nm, enabling the use of UVRRS to selectively study the enzyme-bound substrate without interference from fluorescence. In contrast, the ES complex of 3,4-PCD and PCA could not be studied using visible resonance Raman due to the strong fluorescence of the complex.[27]

The spectroscopic data presented in this study provide direct, unequivocal evidence that an extradiol dioxygenase, DHBD, binds its preferred substrate, DHB, as a monoanion. This is corroborated by the observed asymmetric binding of DHB to DHBD ($r_{Fe-O} = 2.0$ and 2.4 Å; Table 3), which indicates that O2 is deprotonated, but not O3. These results substantiate spectroscopic data that had been interpreted to indicate this state of protonation of the substrate in the ES complex. Thus, XAS data of C23O (catechol 2,3-dioxygenase):catechol complex indicated that there are five N/O scatters coordinated to the Fe(II): four at 2.10 Å and one at 1.93 Å.[13] The short distance was attributed to the asymmetric binding of catechol, suggesting that the latter is bound as a monoanion, as observed in [Fe(II)(6TLA)(DBCH)](ClO_4), a well-characterized mononuclear Fe(II)·catechol model compound.[77] Interestingly, the asymmetry of DHB binding in a complex with a reactivated homologue does not appear to be as significant ($r_{Fe-O} = 2.02$ and 2.25 Å).[12] Finally, UV/Vis Absorption spectroscopy had indicated that 4-nitrocatechol binds to C23O as a monoanion.[28] However, as 4-nitrocatechol is a poor substrate of C23O, its mode of binding may not reflect that of good substrates.

The initial step of the proposed catalytic mechanism of extradiol dioxygenases is bidentate binding of the catecholic substrate to the ferrous center as a monoanion (Figure 10).[1−3] The Lewis acidity of the Fe(II) should assist in the deprotonation of the substrate. Nevertheless, a recent model reaction study suggested that a base was required for substrate monodeprotonation and an acid was required for the subsequent Criegee rearrangement.[30] The structural data strongly suggest that the conserved active site His241 of DHBD assists in the deprotonation of the catechol in the enzyme-catalyzed reaction. As described above, the substrate-induced structural changes observed for His241 are consistent with its protonation. It is further noted that Tyr250 could act as a proton shuttle between the catecholic substrate and His241.

In the subsequent step of the proposed mechanism, O_2 binds to the ferrous iron. As shown in Figure 10, the dominant form of this species would be Fe(III)$-O_2^{-\bullet}$. Formation of Fe(III) would induce deprotonation of the 3-hydroxyl, forming the dianion chelate, as proposed in intradiol enzymes.[22,24,27] The proton could be picked up by the iron-bound superoxide. Interestingly, Nϵ2 of the conserved His195 is positioned within 3 Å of the proximal O atom in the modeled DHBD:DHB:O_2 ternary complex,[78] and could thus stabilize protonation of that particular O atom of the superoxide species. Electron transfer from the bound catechol would produce an Fe(II)−semiquinone. Attack of the activated oxygen species in a pseudoaxial position at C-2 satisfies the orbital steering requirements proposed by Bugg to be critical for extradiol cleavage.[3] In the subsequent step, the proton originating from the 3-hydroxyl group would assist in the heterolysis of the O−O bond in the proposed Criegee rearrangement that results in the lactone and the Fe-hydroxide. Finally, hydrolysis of the lactone by the Fe-bound hydroxide, and release of the proton on His241 complete the catalytic cycle. This mechanism, which is summarized in Figure 10, does not rule out alternate roles for His195 and His241. However, it illustrates the importance of the Fe(II)-bound monoanion in coordinating electron and proton transfer upon O_2 binding.

For intradiol dioxygenases, it is generally accepted that the substrate binds as a dianion, and that the displaced tyrosyl and hydroxide ligands accept the two hydroxyl protons.[79] The

(76) Addison, A. W.; Rao, T. N.; Reedijk, J.; van Rijn, J.; Verschoor, G. C. *J. Chem. Soc., Dalton Trans.* **1984**, *1984*, 1349−1356.

(77) Chiou, Y.-M.; Que, L., Jr. *Inorg. Chem.* **1995**, *34*, 3577−3578.

(78) Bolin, J. T.; Eltis, L. D. In *Handbook of Metalloproteins*; Messerschmidt, A., Huber, R., Poulos, T., Wieghardt, K., Eds.; John Wiley & Sons: New York, 2001; pp 632−642.

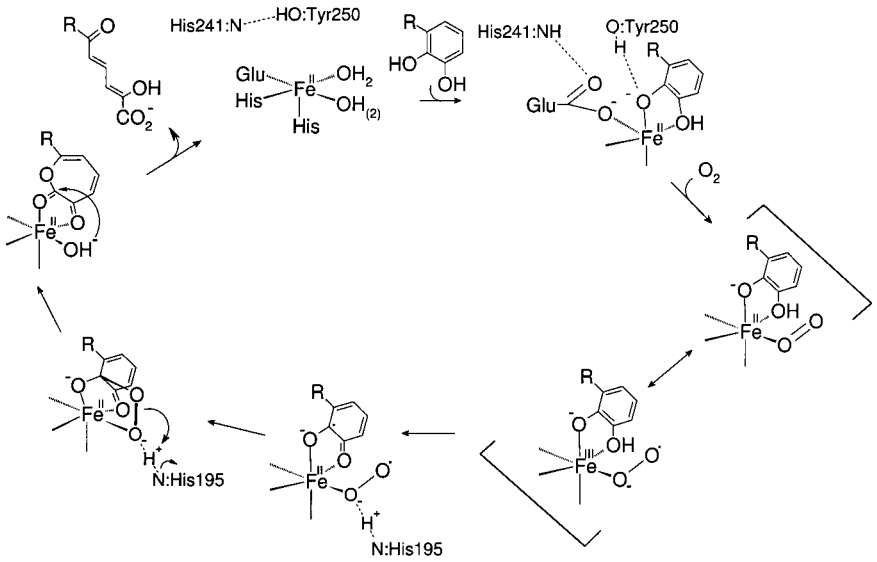

Figure 10. Proposed mechanism of extradiol dioxygenases (adapted from[3,13]). The role of conserved active site residues is proposed. For clarity, the displacement of solvent species from the ferrous center is not depicted explicitly.

protonation state of the substrate is largely based on crystallographically determined bond lengths, which indicate that the substrate is asymmetrically bound: the long Fe−O bond is trans to a tyrosinate ligand and the short Fe−O bond is trans to a neutral histidine ligand.[22,24,25] The asymmetry is proposed to reflect ketonization of the bond trans to the tyrosine. A survey of the structures in the database (3PCA, 1EOB, 1DLT) reveals that the Fe−O bond lengths are similar to those observed in ES complexes of extradiol enzymes ($r_{Fe-O} = 2.0 \pm 0.1$ Å and 2.4 ± 0.2 Å). Visible resonance Raman studies using the ligand-to-metal charge transfer (LMCT) bands show that 4-nitrocatechol and 3,4-dihydroxyphenylacetate bind to 3,4-PCD as dianions.[27,29] UV/Vis absorption spectroscopy corroborates dianionic binding of 4-nitrocatechol to 3,4-PCD and C12O.[28] 4-Nitrocatechol is an inhibitor of 3,4-PCD and 3,4-dihydroxyphenylacetate is a very poor substrate. Thus, these analogues may not bind in the same manner as the preferred substrate of the enzyme, PCA. However, structural data indicate that 3,4-PCD binds 3,4-dihydroxyphenylacetate and PCA in a similar manner. Considering the proposed importance of dianionic binding of the substrate to substrate activation in the catalytic mechanism of intradiol enzymes,[22] it would be useful to obtain direct evidence for the protonation state of the bound substrate using UVRRS.

Acknowledgment. F.H.V. and C.J.B. contributed equally to this work. This work was supported in part by grants from the Natural Sciences and Engineering Research Council of Canada (NSERC), the Canada Foundation for Innovation (CFI), the British Columbia Health Research Foundation (BCHRF), and the National Institutes of Health (NIH grant GM-52381 to J.T.B.). F.H.V. was the recipient of Li Tze Fong Memorial and NSERC scholarships. C.J.B. was the recipient of an NSERC scholarship. Geneviève Labbé is thanked for her assistance in the titration of catechols. Dr. Alina Kulpa is thanked for her assistance with the construction of the fiber optic probes. Dr. Seungil Han is thanked for his considerable contributions to the crystallographic studies.

(79) Orville, A. M.; Lipscomb, J. D. *Biochemistry* **1997**, *36*, 14044−14055.

JA0174682